Electronic Supplementary Material (ESI) for New Journal of Chemistry.

Supporting information

Disposable Tartrazine Sensor Fabricated with Synchronously Activated Nanocomposite Comprising Gadolinium Molybdate Nanoflowers Anchored Functionalized Carbon Nanofibers

Abishek Jayapaul [1], Rajalakshmi Sakthivel [1], Yu-Chien Lin [1], Udesh Dhawan [2], Xinke Liu [3,4], Hsiao-Wei Wen [5,6], Ren-Jei Chung [1,7,*]

[1] Department of Chemical Engineering and Biotechnology, National Taipei University of Technology (Taipei Tech), Taipei 10608, Taiwan

[2] Centre for the Cellular Microenvironment, Division of Biomedical Engineering, James Watt School of Engineering, Mazumdar-Shaw Advanced Research Centre, University of Glasgow, Glasgow G116EW, UK

[3] College of Materials Science and Engineering, Chinese Engineering and Research Institute of Microelectronics, Shenzhen University, Shenzhen 518060, China

[4] Department of Electrical and Computer Engineering, National University of Singapore, Singapore 117583, Singapore

[5] Department of Food Science and Biotechnology, National Chung Hsing University, Taichung 402202, Taiwan

[6] Food and Animal Product Safety Inspection Center, National Chung Hsing University, Taichung 402202, Taiwan

[7] High-value Biomaterials Research and Commercialization Center, National Taipei University of Technology (Taipei Tech), Taipei 10608, Taiwan

***Correspondence to:** Department of Chemical Engineering and Biotechnology, National Taipei University of Technology (Taipei Tech), No. 1, Section 3, Zhongxiao E. Rd., Taipei 10608 Taiwan.

E-mail addresses: rjchung@ntut.edu.tw (R.-J. Chung)

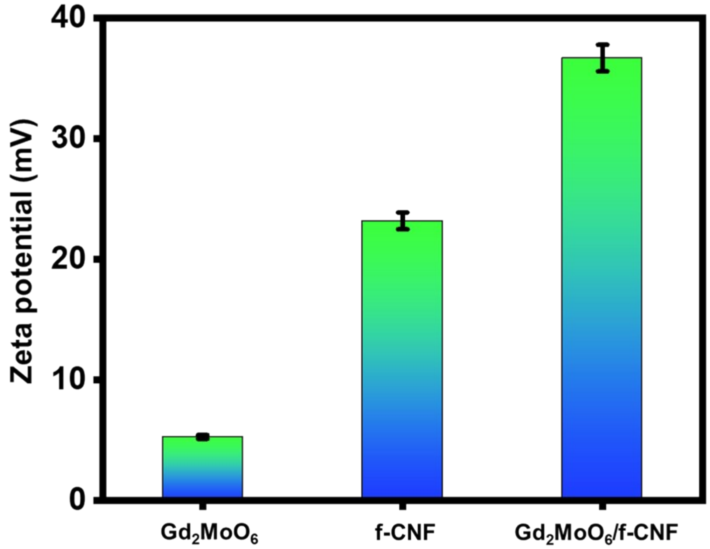

Fig. S1. Zeta potential of different modified electrodes

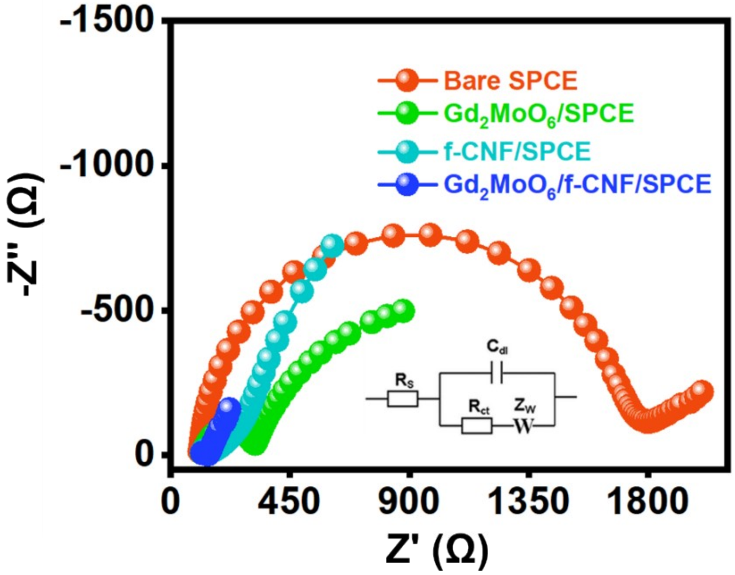

Fig. S2. (A) EIS spectra for different electrodes (Bare and modified) performed in $[Fe(CN)_6]^{3-/4-}$in 0.1 M KCl as electrolyte; (inset) Randel's equivalent circuit in EIS studies.

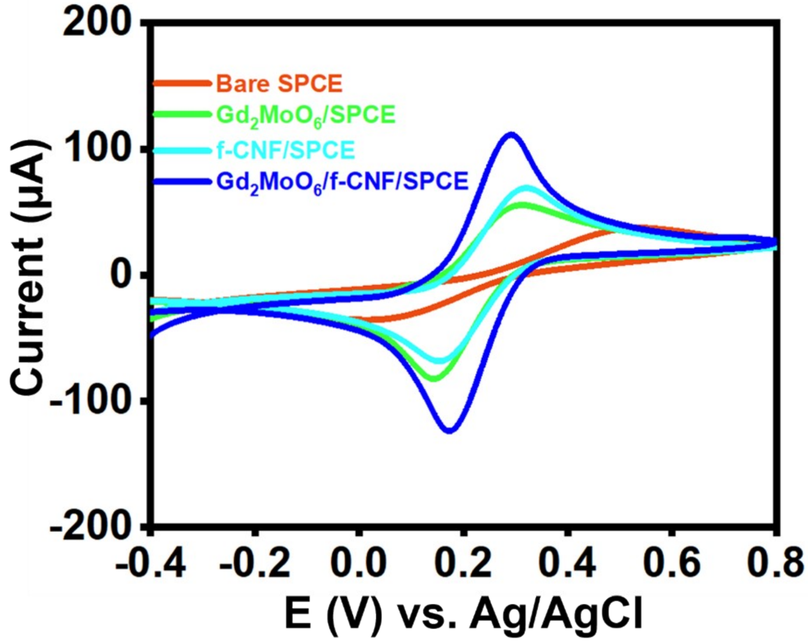

Fig. S3. (A) CV curves for different electrodes (Bare and modified) performed in $[Fe(CN)_6]^{3-/4-}$in 0.1 M KCl as electrolyte.

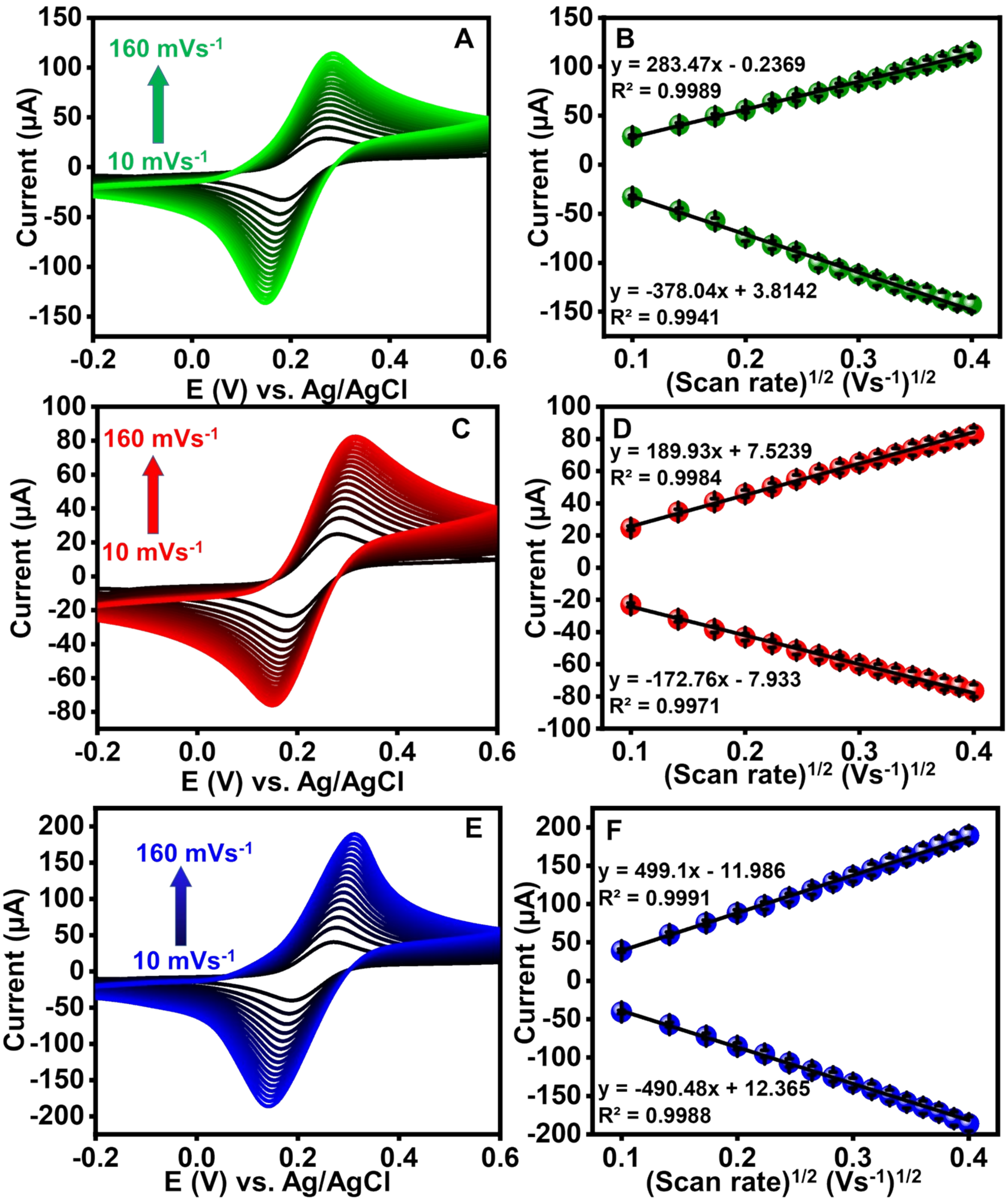

Fig. S4. CV profile obtained by varying scan rates from 0.02-0.2 Vs^{-1} at (A) Gd_2MoO_6/SPCE, (C) f-CNF/SPCE, and (E) Gd_2MoO_6/f-CNF/SPCE; (B, D, and F) corresponding calibrated plot of the square root of scan rate versus anodic and cathodic peak currents; All the above experiments were performed in $[Fe(CN)_6]^{3-/4-}$in 0.1 M KCl as electrolyte.

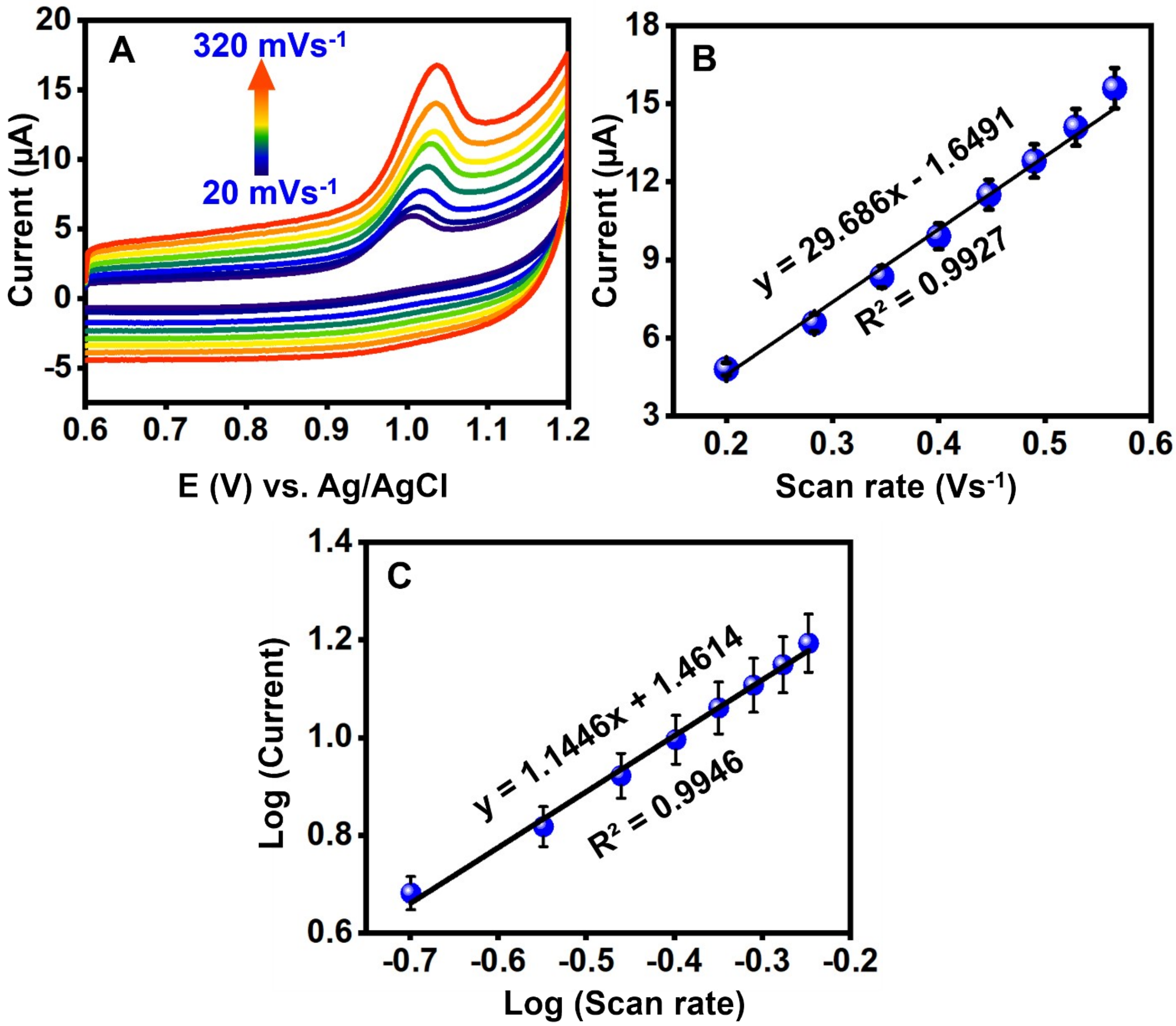

Fig. S5. (A) CV profile obtained by varying scan rates from 0.02-3.2 Vs^{-1} at Gd_2MoO_6/f-CNF/SPCE; (B) Calibrated plot of the scan rate versus anodic peak currents; (C) log of scan rates versus log of peak currents; All the above experiments were performed in 0.1 M PB as electrolyte.

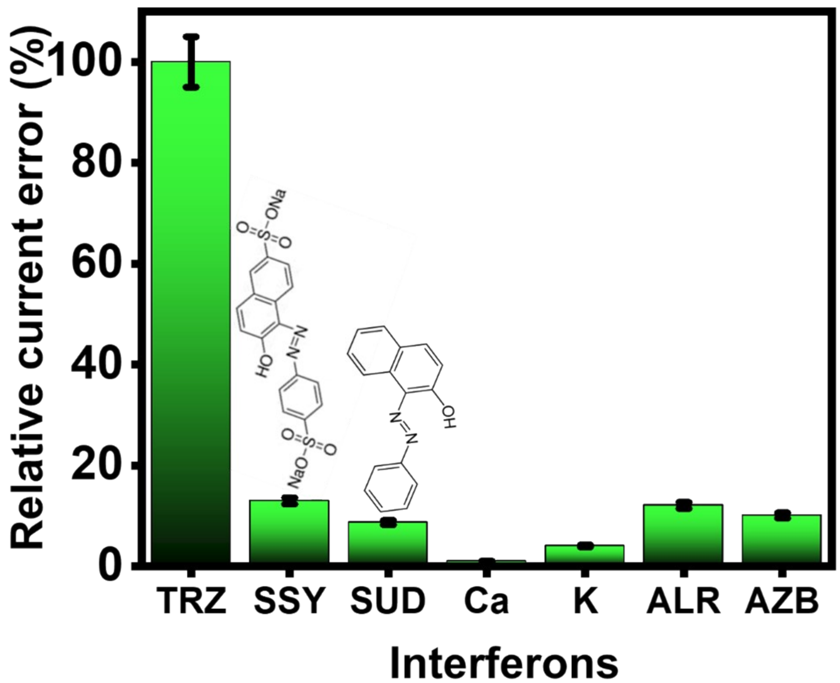

Fig. S6. Plot of interferents versus corresponding relative current error percentage.

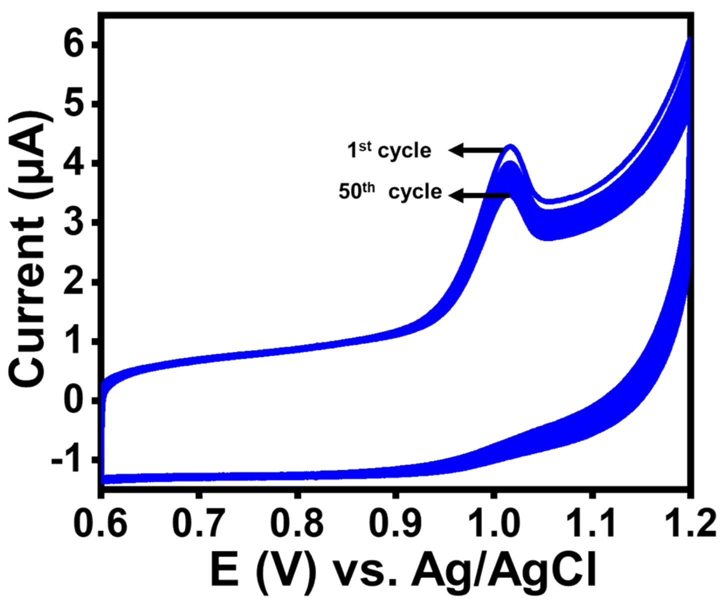

Fig. S7. Functional stability of Gd_2MoO_6/f-CNF/SPCE analyzed over 50 continuous CV cycles.

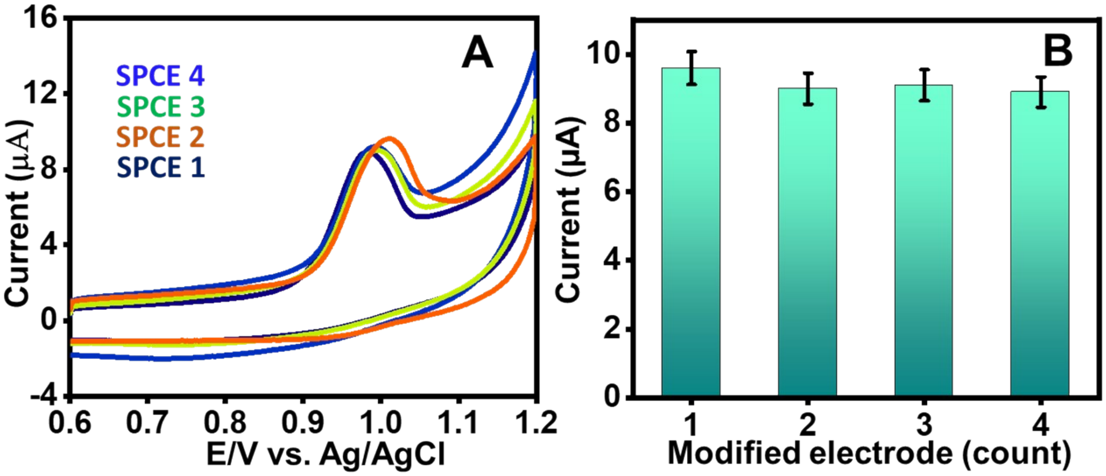

Fig. S8. (A) CV curves obtained for different SPCE coated with Gd_2MoO_6/f-CNF composite; (B) Calibrated plot of the modified electrodes versus relative current.

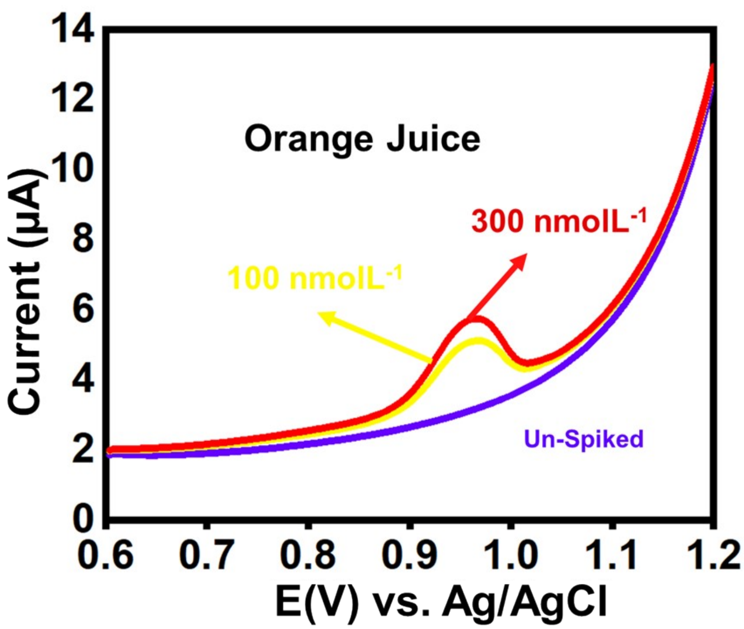

Fig. S9. DPV plot of spiked and un-spiked addition of TRZ in orange juice sample.

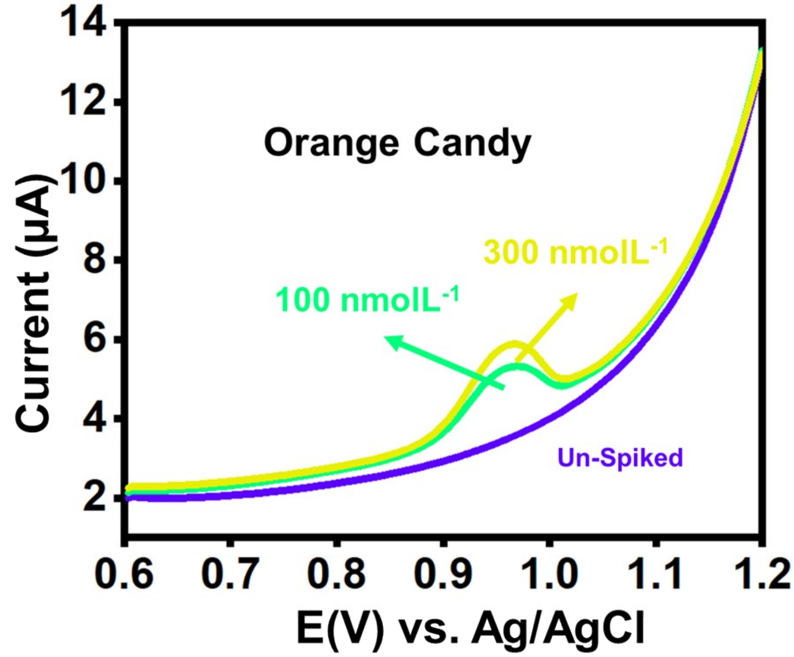

Fig. S10. DPV plot of spiked and un-spiked addition of TRZ in orange candy sample.

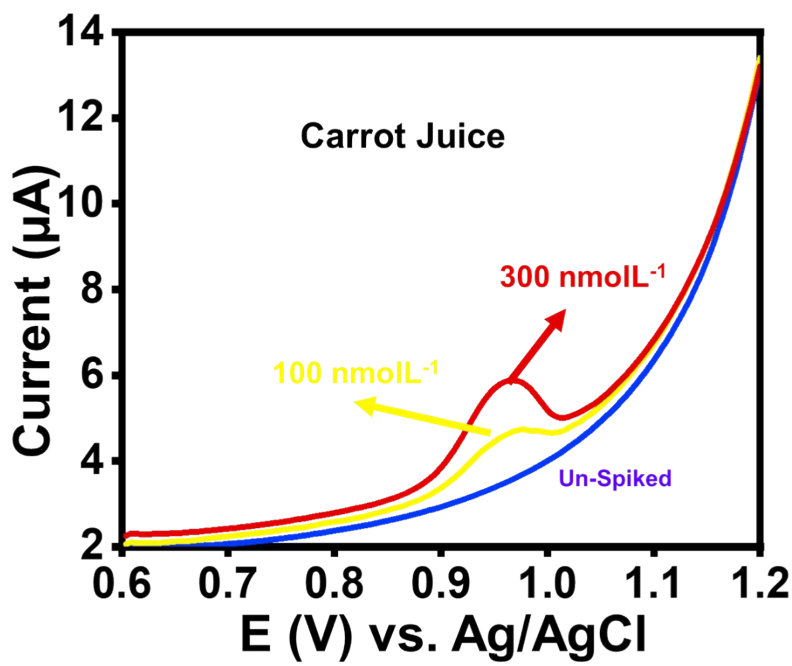

Fig. S11. DPV plot of spiked and un-spiked addition of TRZ in carrot juice sample.

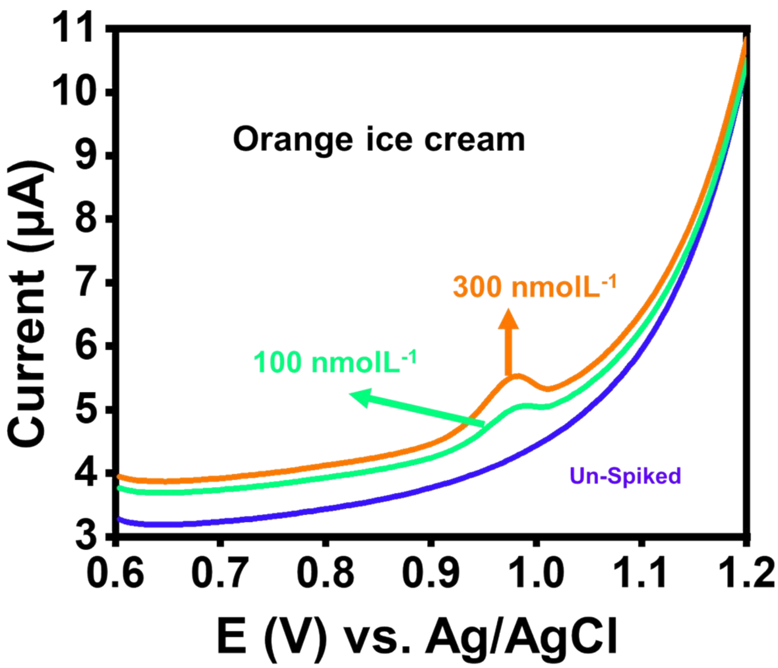

Fig. S12. DPV plot of spiked and un-spiked addition of TRZ in orange ice-cream sample.

Table S1: Recovery estimation table for real sample analysis.

Sample	Added ($nmolL^{-1}$)	Found DPV ($nmolL^{-1}$)	GC-MS	Recovery (%)		RSD (±%)	
				DPV	GC-MS	DPV	GC-MS
Orange juice	0	0	0	0	0	-	-
	100	93	91.21	93	91.21	1.69	2.94
	300	272	260.88	90.7	88.6	1.11	2.20
Orange candy	0	0	0	0		-	-
	100	103.3	99.89	103.3	99.89	2.44	2.91
	300	296.8	291.6	98.93	97.2	1.91	2.12
Carrot juice	0	0		0	0	-	-
	100	96.3	93.7	96.3	93.7	2.31	2.77
	300	279.4	263.3	93.1	87.7	2.17	2.46
Orange ice cream	0	0	0	0	0	-	-
	100	97.4	96.84	97.4	94.84	3.11	3.64
	300	283.6	276.73	94.5	92.2	2.92	3.34